CHAPTER IV
RESULTS AND DISCUSSION

4.1 Catalytic Characterization

4.1.1 Atomic Absorption Spectroscopy (AAS)

The actual metal loading of the Zn and Ga on the HZSM-5 (30) catalysts were determined by atomic absorption spectroscopy (AAS). Table 4.1 shows the amount of Zn and Ga contents in HZSM-5 catalysts, prepared by incipient wetness impregnation (IWI) method. The results indicated that the amount of Ga and Zn remained invariant compared to the expected metal loadings in the catalysts.

Table 4.1 The actual and expected metal loading of the catalysts

Catalysts	*Actual metal loading (wt%)
HZSM-5 (30)	-
1Ga/HZSM-5	0.93
3Ga/HZSM-5	2.75
5Ga/HZSM-5	5.14
7Ga/HZSM-5	6.39
1Zn/HZSM-5	0.91
3Zn/HZSM-5	2.92
5Zn/HZSM-5	4.83
7Zn/HZSM-5	6.38

*Using atomic absorption spectroscopy (AAS)

4.1.2 N_2 Adsorption/Desorption Measurements (BET Analysis)

Brunauer-Emmett-Tellet (BET) technique was used to determine surface area of the catalysts. The surface area of the parent HZSM-5 with different SiO_2/Al_2O_3 ratios and modified HZSM-5 catalysts are summarized in Table 4.2. The

surface area of parent HZSM-5 zeolites decreased in the following order: HZSM-5 (30) > HZSM-5 (50) > HZSM-5 (23).

The introduction of Zn and Ga on HZSM-5 catalysts resulted in the decrease in surface area of Zn/HZSM-5 and Ga/HZSM-5 catalysts. Table 4.2 shows the comparable surface area of parent HZSM-5 (30) with the small amount of metal loading over HZSM-5 catalysts (1Zn/HZSM-5, 1Ga/HZSM-5, 3Ga/HZSM-5). This results indicated the highly dispersed of Zn and Ga over HZSM-5 zeolites. However, it was also noticed that the surface area of Zn/HZSM-5 and Ga/HZSM-5 catalysts decreased with further increase of metal loadings. The significant loss in surface area of 7Zn/HZSM-5 catalyst was due to the high amount of metal loading which partially blocked the pore of HZSM-5 zeolite. The Ga-doped HZSM-5 catalysts only slightly reduced the surface area of catalysts. These results indicated that the Ga incorporated was mostly dispersed outside the pore of HZSM-5 as gallium oxide clusters (Ga_2O_3) (Ausavasukhi, A., 2009). Agreed with previous work, the incipient wetness impregnation method did not allow the large hydrated Ga^{3+} cations passed the pore system of HZSM-5 and entered the zeolite framework position (except a minority healing lattice defects by incorporation) (Guisnet, M., 1992).

Table 4.2 Textural properties of the parent HZSM-5 catalysts and modified HZSM-5 catalysts

Catalyst	SiO_2/Al_2O_3	S_{BET} (m^2/g_{cat})
HZSM-5	23	334.2
HZSM-5	30	375.7
HZSM-5	50	356.3
1Zn/HZSM-5	30	334.0
3Zn/HZSM-5	30	309.6
5Zn/HZSM-5	30	295.6
7Zn/HZSM-5	30	283.5
1Ga/HZSM-5	30	353.2
3Ga/HZSM-5	30	333.8
5Ga/HZSM-5	30	327.4
7Ga/HZSM-5	30	322.6

4.1.3 X-ray Diffraction (XRD)

To confirm the zeolitic structure and crystallinity of the catalysts, XRD was applied to investigate the structure of modified HZSM-5 catalysts. As shown in Figures 4.1 and 4.2, Zn/HZSM-5 and Ga/HZSM-5 zeolites exhibited similar characteristic peaks of MFI structure. This confirmed that the framework structure of HZSM-5 zeolites remained intact after the modification.

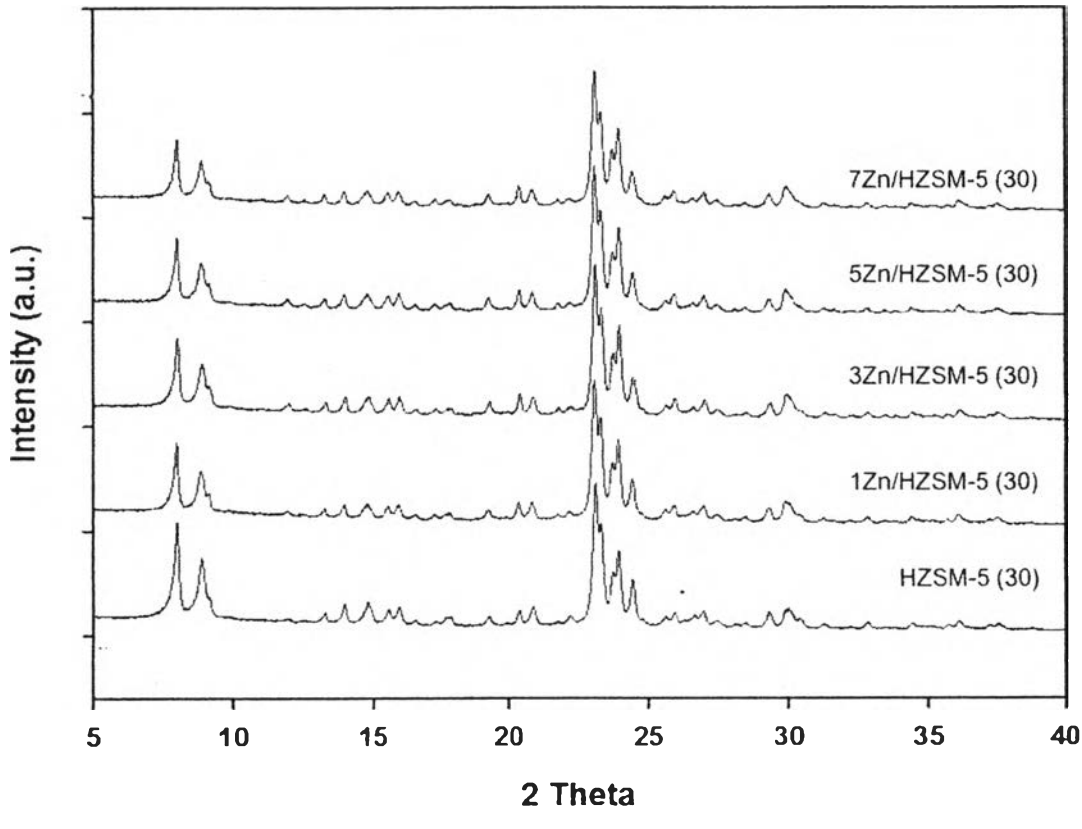

Figure 4.1 XRD patterns of Zn/HZSM-5 catalysts prepared by incipient wetness impregnation (IWI) method.

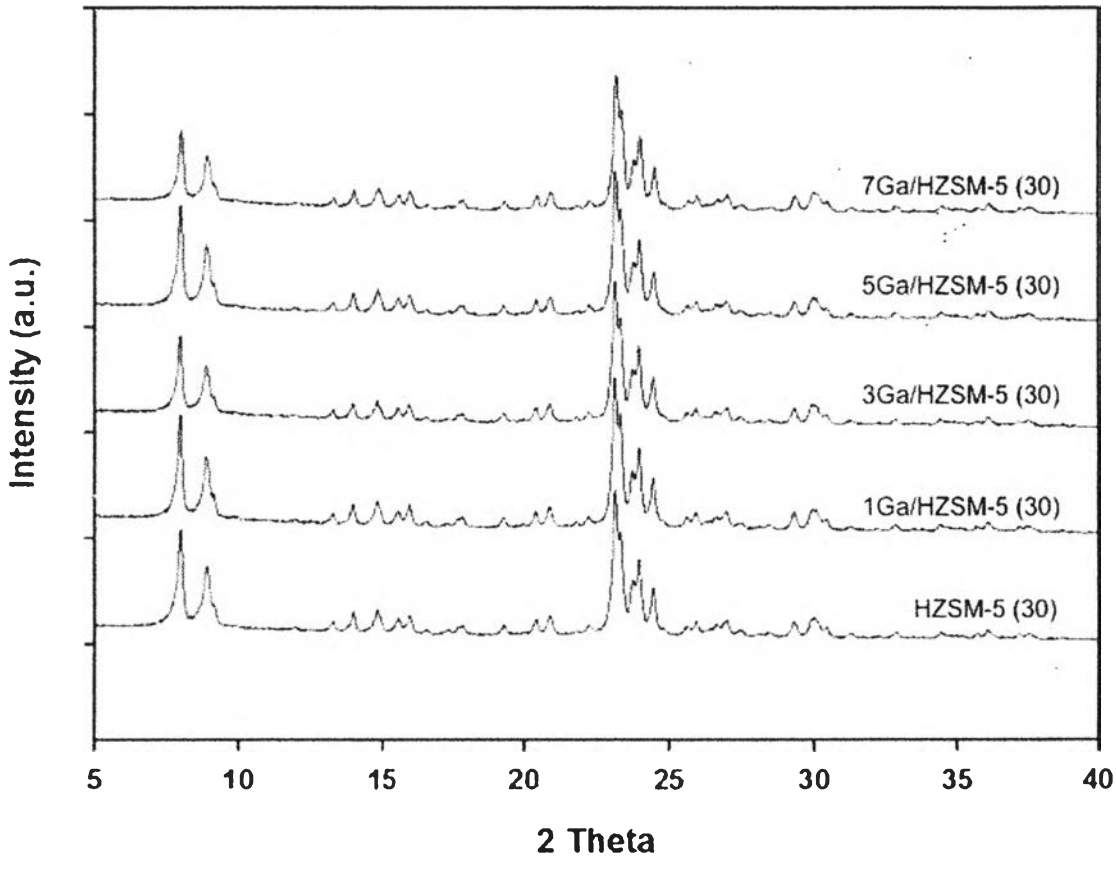

Figure 4.2 XRD patterns of Ga/HZSM-5 catalysts prepared by incipient wetness impregnation (IWI) methods.

4.1.4 Temperature Programmed Reduction (TPR)

In order to determine the reduction behaviour of the catalysts, the H_2 temperature programmed reduction (TPR) of Ga/HZSM-5 catalysts were performed in the temperature range from 30 °C to 800 °C. The TPR profiles of the Ga/HZSM-5 catalysts are shown in Figure 4.3. It can be observed that all samples had a reduction peak at 550-660 °C, which is the reduction of well-dispersed Ga species such as a small Ga_2O_3 particles and GaO_+ species interacting with the zeolite (Artit, A., 2014). In addition, the H_2 consumption peak near 700-760 °C of 5Ga/HZSM-5 and 7Ga/HZSM-5 indicated that the Ga species agglomerated at higher loading into larger Ga_2O_3 clusters, and probably segregated to the outer surface of HZSM-5 (Artit, A., 2014).

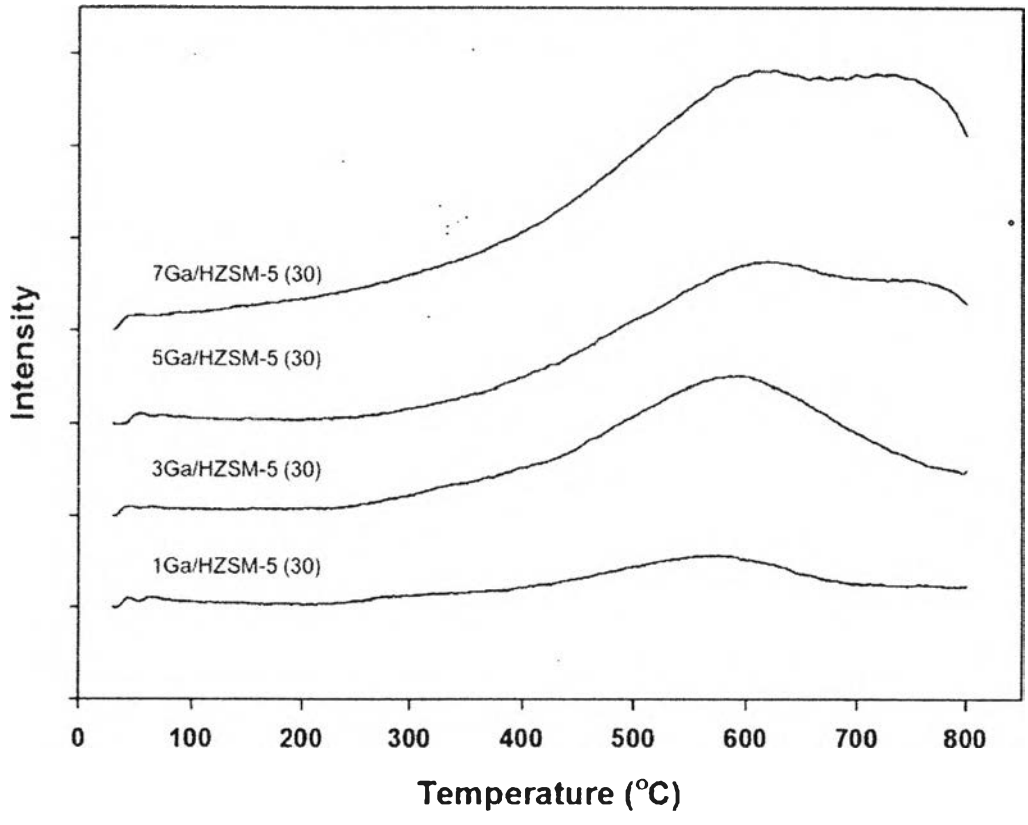

Figure 4.3 TPR-H_2 profiles of Ga/HZSM-5 catalysts with different Ga loading.

4.1.5 Temperature Programmed Desorption (TPD) of Isopropylamine

The isopropylamine temperature programmed desorption (IPA-TPD) was used to quantify the remaining of Brønsted acid sites, as it is a well-known technique allowing us to monitor the desorbed ammonia and propylene from decomposition of isopropylamine over Brønsted acid (Hofmann elimination reaction). Figure 4.4 shows the TPD profiles of desorbed propylene (*m/e* = 41) related to temperature, which depends on the acid strength. The desorption peak at 80 °C to 120 °C, represented to the physical desorption of unreacted IPA from weak acid sites (Elena, A.F., 2010). The peak at 350 °C is the quantification of the strong Brønsted acid sites (Artit, A., 2009). As compared with the different SiO_2/Al_2O_3 of parent HZSM-5, the Figure 4.4 shows that HZSM-5 catalyst with lower SiO_2/Al_2O_3 has higher Brønsted acid sites than higher one.

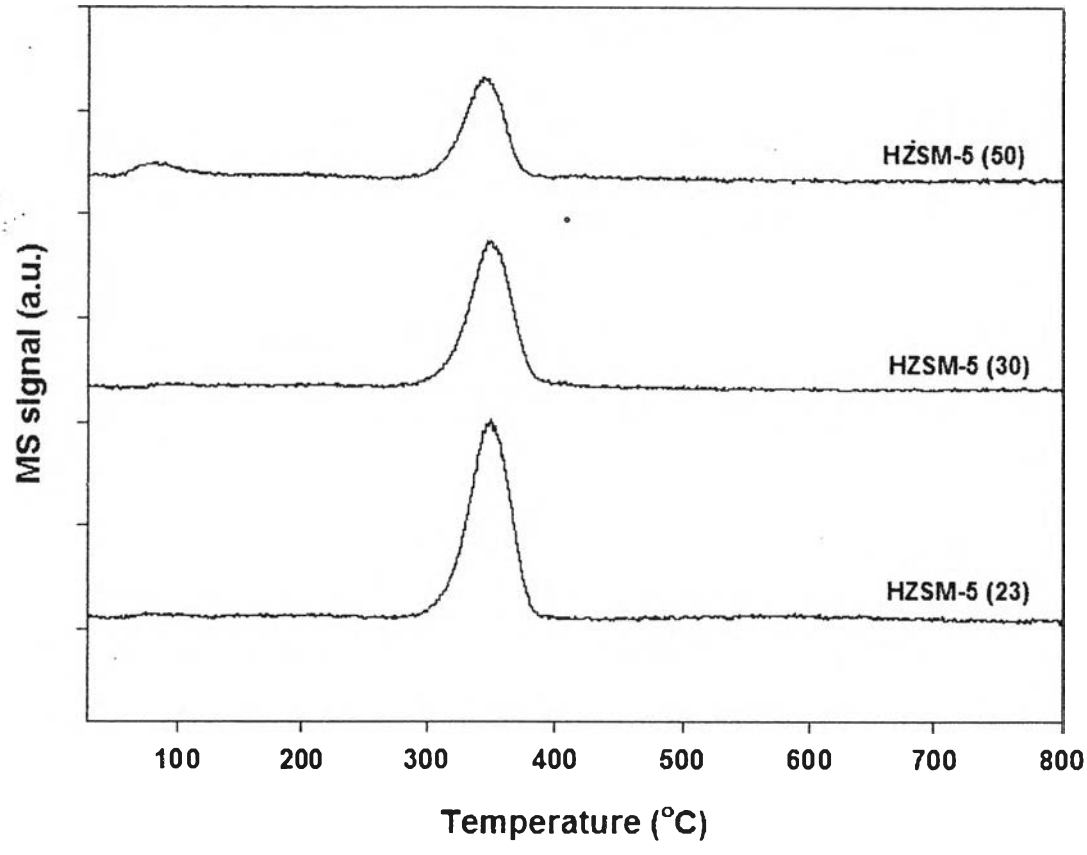

Figure 4.4 Isopropylamine-TPD profiles of parent HZSM-5 catalysts. The mass monitored was propylene (*m/e* = 41).

Figure 4.5 shows the TPD profiles of Zn/HZSM-5 catalysts. Compared to the parent HZSM-5 (30), the significant decrease in the strong Brønsted acid sites after loading Zn was also observed. The strong Brønsted acid sites decreased from 376.8 μmol/g_{cat} for HZSM-5 (30) to 233.6 μmol/g_{cat} for 1Zn/HZSM-5. It indicates that the incorporation of bivalent Zn cations preferentially exchanged with protons of strong Brønsted acid sites of HZSM-5 (Yu, L., 2012). It is interesting to note that the further increase in Zn loading from 5Zn/HZSM-5 to 7Zn/HZSM-5 did not result in the decrease of Brønsted acid site. The reason for that might be due to some parts of Zn deposited as extra-framework ZnO species.

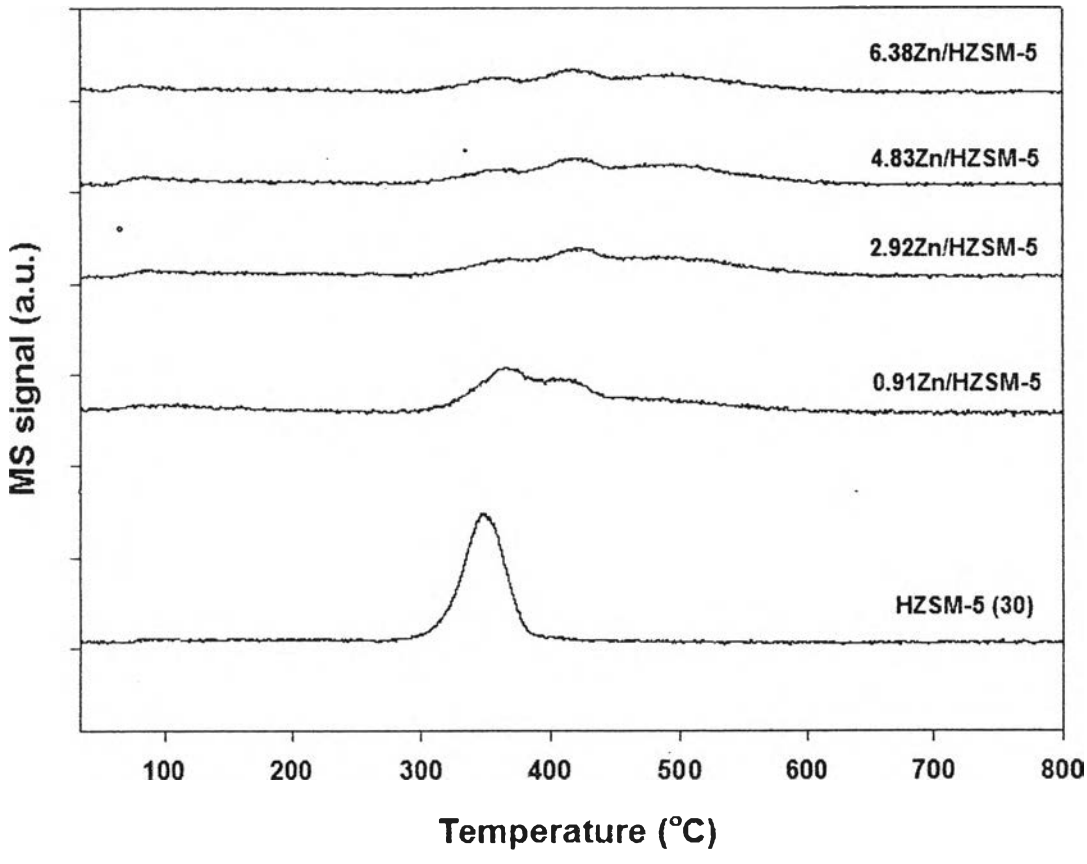

Figure 4.5 Isopropylamine-TPD profiles of Zn/HZSM-5 prepared by IWI. The mass monitored was propylene (*m/e* = 41).

The effect of Ga loading to the strong Brønsted acidity of parent HZSM-5 is shown in Figure 4.6 and Table 4.3. It was noticed that the strong Brønsted acid site were hardly decreased by increase metal loading. Since the prepared catalysts were calcined without reduction process, the Ga incorporated is mostly retained in form of isolated oxide clusters (Ga_2O_3) without exchanged with the strong Brønsted acid site (Ausavasukhi, A., 2009).

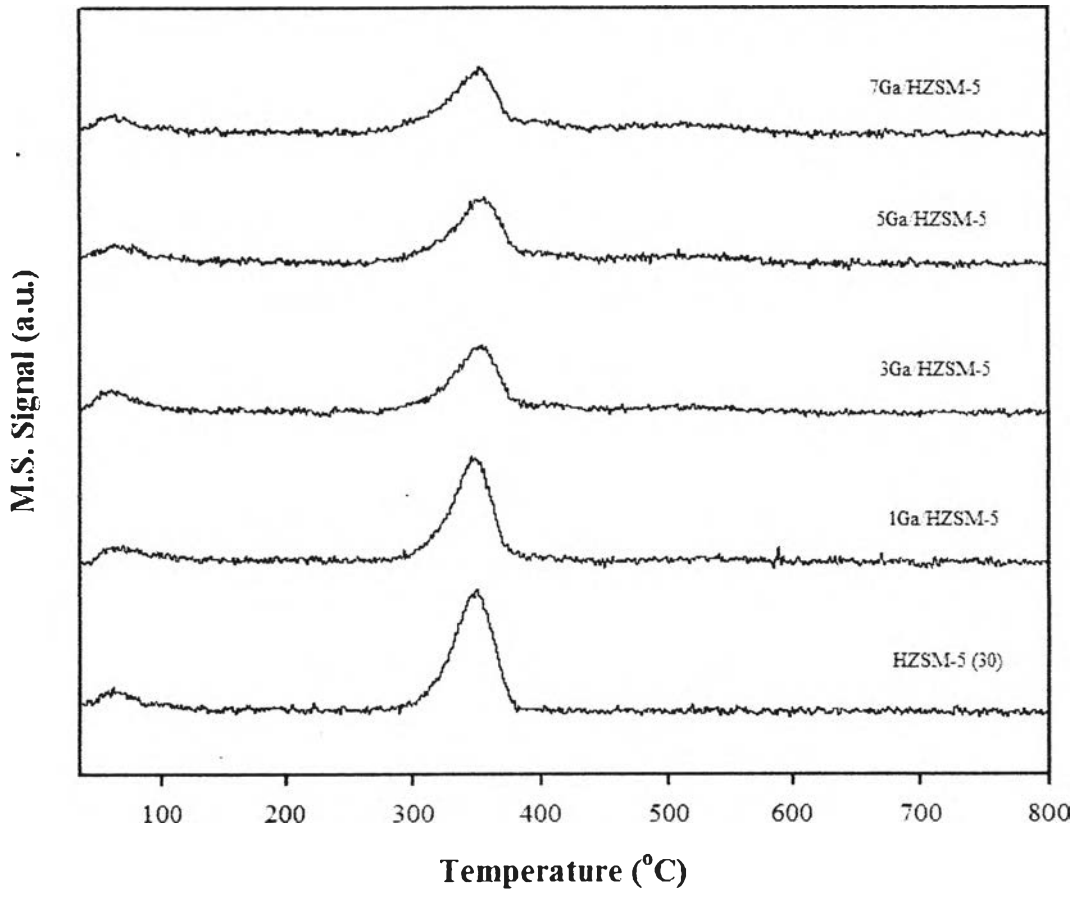

Figure 4.6 Isopropylamine-TPD profiles of Ga/HZSM-5 prepared by IWI. The mass monitored was propylene (*m/e* = 41).

Table 4.3 The strong Brønsted acid site of the parent HZSM-5, Zn/HZSM-5, and Ga/HZSM-5 catalysts from TPD of isopropylamine

Catalysts	Strong Brønsted acid site ($\mu mol/g_{cat}$)
HZSM-5 (23)	434.5
HZSM-5 (30)	376.8
HZSM-5 (50)	261.3
1Zn/HZSM-5	233.6
3Zn/HZSM-5	127.4
5Zn/HZSM-5	99.6
7Zn/HZSM-5	97.28
1Ga/HZSM-5	335.7
3Ga/HZSM-5	306.8
5Ga/HZSM-5	288.8
7Ga/HZSM-5	263.3

4.1.6 X-ray Photoelectron Spectroscopy (XPS)

The XPS spectra of Zn/HZSM-5 catalysts is illustrated in Figure 4.7. By fitting the XPS spectra, Zn/HZSM-5 catalyst showed 2 types of Zn species. It is reasonable to indicate the higher binding energy (1023.5 eV for 1Zn/HZSM-5, 1023.3 eV for 3Zn/HZSM-5, 1023.5 eV for 5Zn/HZSM-5, and 1023.9 eV for 7Zn/HZSM-5) as $Zn(2p_{3/2})$ binding energy for bivalent Zn cations stabilized at exchanged site, as lattice oxygens of the zeolite have a higher electronegativity than O^{2-} group (Tamiyakul, S., 2015). The presence of ZnO on 1Zn/HZSM-5, 3Zn/HZSM-5, 5 Zn/HZSM-5, and 7Zn/HZSM-5 can be involved by the presence of peak at 1022.6, 1022.3, 1022.1, and 1022.6 eV, respectively. Compared to ZnO reference (1021.8 eV), the shifting to higher binding energy is due to the effect of HZSM-5 framework (Tamiyakul, S., 2015). Table 4.4 showed that the increase of Zn loading, the exchangeable Zn^{2+} species was comparable while the ZnO species trend to increase. During preparation by IWI techniques, we obtain less than 50% of the full exchange capacity (Cabrera, I.M., 2006). When we reach the maximum limitation of exchange capacity, the further increase in Zn loading did not result in

increase of bivalent Zn cations at the exchange site. On the other hand, the XPS results showed that in the case of greater amount of Zn loading resulted in higher amount of ZnO species. The result clearly explained the reason why increasing the metal loading, the surface area of catalyst was reduced (Table 4.2).

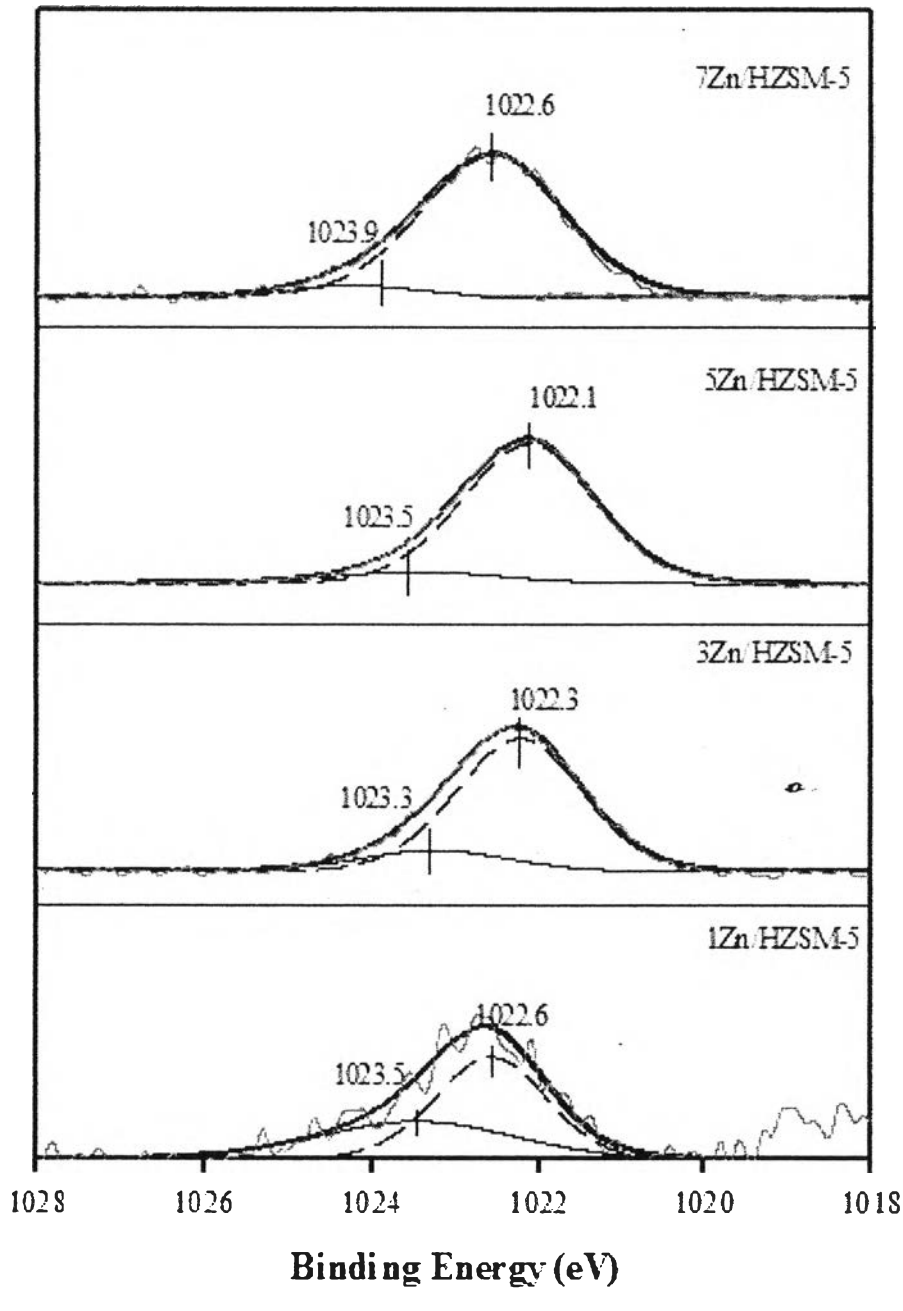

Figure 4.7 XPS spectra of Zn ($2p_{3/2}$) of 1Zn/HZSM-5, 3Zn/HZSM-5, 5Zn/HZSM-5, and 7Zn/HZSM-5.

Table 4.4 The quantitative of Zn species over Zn/HZSM-5 catalysts

Catalyst	Exchangeable Zn^{2+} species (wt%)	ZnO species (wt%)
1Zn/HZSM-5	0.40	0.60
3Zn/HZSM-5	0.47	2.53
5Zn/HZSM-5	0.48	4.52
7Zn/HZSM-5	0.41	6.59

Figure 4.8 demonstates the XPS spectra of Ga/HZSM-5 catalysts. By fitting the XPS spectra, Ga/HZSM-5 catalysts exhibited 1 type of Ga that was Ga_2O_3. The XPS results confirmed the reason why IPA-TPD of Ga/HZSM-5 catalysts (Table 4.3) barely decreased the strong Brønsted acid site. The Ga incorporated remained in form of isolated oxide clusters without exchanged with the strong Brønsted acid site. As compared to Ga_2O_3 reference (1118.0 eV), the shift to higher binding energy is due to the effect of HZSM-5 framework.

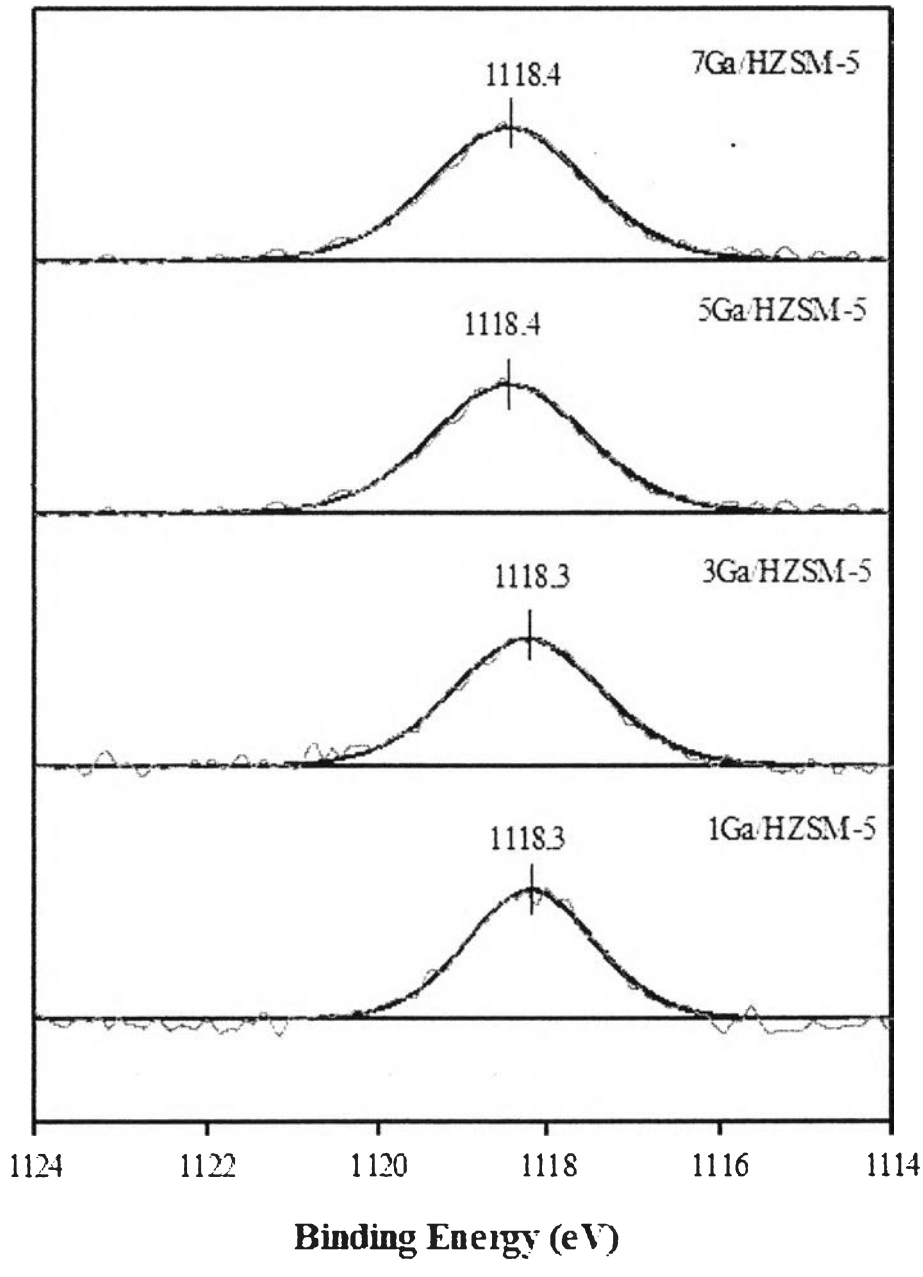

Figure 4.8 XPS spectra of Ga ($2p_{3/2}$) of 1Ga/HZSM-5, 3Ga/HZSM-5, and 5Ga/HZSM-5.

4.2 Catalytic Activity Testing

The parent HZSM-5 and modified catalysts were tested for their catalytic activity and yield in coverting palm fatty acid distillate (PFAD) to petrochemical aromatics. The products can be classified into three main groups; (1) light paraffins:

methane, ethane, propane, butane, and pentane. (2) light olefins: ethylene, propylene, and butene. (3) BTEX: benzene, toluene, ethlybenzene, and xylene.

4.2.1 Proposed Reaction Pathway for Transformation PFAD to Aromatics

Figure 4.9 shows the products yield of palm fatty acid distillate (PFAD) conversion over HZSM-5 (30) as a function of space time (W/F) at 500 °C and 1 atm. From the analysis of the product distribution, the reaction pathways for transformation of PFAD to aromatics over HZSM-5 (30) were proposed in Fig 4.10. Under high temperature, PFAD was first deoxygenated via α and β scissions (Yuhan Yang *et al.*, 2012). As reported by Kissin and coworkers, the effect of electrophilic of carboxyl group induced the scission of fatty acid carbon chain following the catalytic cracking carbenium theory (Y.V. Kissin., 2001 and F.C. Jentoft., 1997). The α–C and β–C are the most active positions, which would generate heavy hydrocarbons and oxygenates (Yuhan Yang *et al.*, 2012). The heavy hydrocarbons were further cracked into light alkanes and alkenes. The deoxygenation of oxygenates via decarbonylation and decarboxylation led to the formation of CO, water, and CO_2, respectively (Gong *et al.*, 2012). It was assumed that the primary cracking occurs within the internal pore structure of HZSM-5 catalyst (Y.K. Ong., 2010). However, initial fragmentation could occur on the external surface of catalysts followed by diffusion into the pores (Leng, T.Y., 1999). Furthermore, light olefins could undergo oligomerization to produce a mixture of heavier olefins and paraffins. The aromatic hydrocarbons were produced by aromatization, alkylation and isomerization of heavier olefins and paraffins (Y.K. Ong., 2010). Coke was produced by direct condensation of PFAD and polymerization of aromatics.

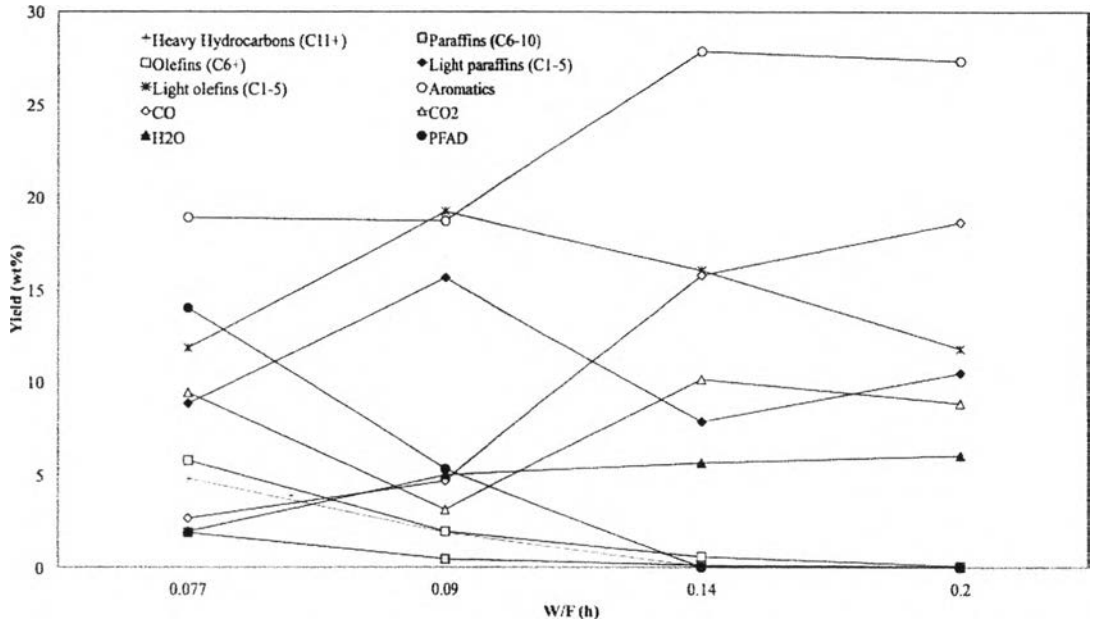

Figure 4.9 Product yield of PFAD conversion over HZSM-5 (30) as a function of space time (W/F) at 500 °C, 1 atm, and TOS = 3 h.

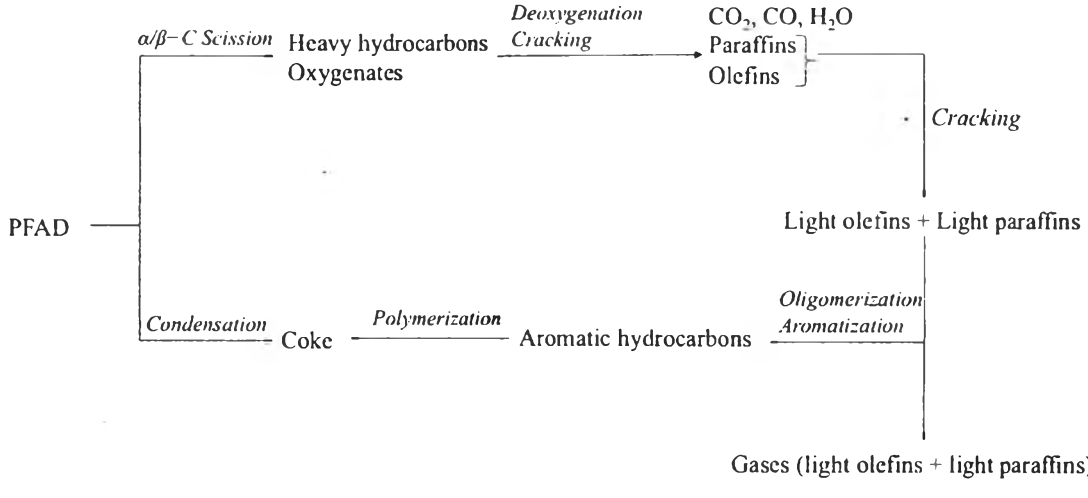

Figure 4.10 Proposed reaction pathway for the conversion of PFAD over HZSM-5 (30) catalyst to hydrocarbon products.

4.2.2 Effect of SiO_2/Al_2O_3 Ratio of HZSM-5 Zeolites

The SiO_2/Al_2O_3 ratios of HZSM-5 zeolites related to its acidity, influencing the transformation of PFAD to aromatics. To investigate the effect of

acid properties, different SiO_2/Al_2O_3 ratios (including 23, 30, and 50) were tested in the aromatization of PFAD at 500 °C under atmospheric pressure. Figure 4.11 shows the conversion and products yield (including aromatics, light paraffins, BTEX, H_2, CO, CO_2, and H_2O) over different SiO_2/Al_2O_3 ratios at third hour time on stream (TOS). The results indicated that the PFAD conversion were almost 100 % for HZSM-5 catalysts which SiO_2/Al_2O_3 ratios of 30 and 50. On the other hand, the PFAD conversion of HZSM-5 (23) was only 83 wt%. The aromatics yield trend to decreased in the following order: HZSM-5 (30) > HZSM-5 (50) > HZSM-5 (23). It is well known that the increase in SiO_2/Al_2O_3 ratio resulted in the decrease of acidity (as shown in Table 4.3), which facilitated the aromatization reaction. Otherwise, the HZSM-5 (23) did not exhibit the highest BTEX yield. This result implied that there must be other factors controlling the catalytic activity for this reaction besides the surface acidity. For acid-dehydration reaction, when water was present as inert co-feeding or product, it could affect the activity and stability over the solid-acid catalysts. The amount of adsorbed water and adsorption strength of water decreased with increasing SiO_2/Al_2O_3 ratio (Kim *et al.*, 2010). The temperature programmed desorption of water (H_2O-TPD) was investigated over HZSM-5 with SiO_2/Al_2O_3 ratios of 23, 30, and 50 as shown in Figure 4.12. It was indicated that HZSM-5 (23) showed the highest desorption temperature and amount of water-desorbed. Therefore, the low aromatization activity of HZSM-5 (23) might be due to its hydrophilicity. Compared with HZSM-5 (30), the lower hydrophilicity and higher in surface area of the catalyst led to the higher in available active site for aromatization reaction.

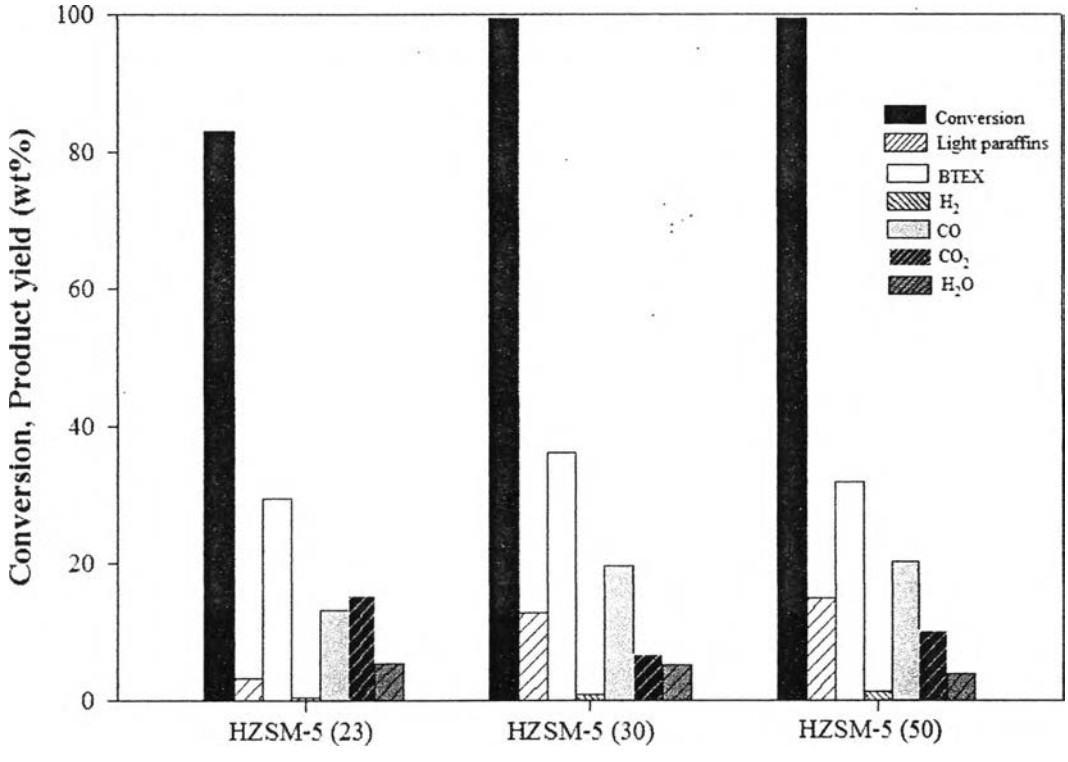

Figure 4.11 Effect of SiO_2/Al_2O_3 ratio of HZSM-5 zeolites on the PFAD conversion, and product yield. *(Reaction conditions: 500 °C under atmospheric pressure, and WHSV= 5 h^{-1}, and TOS = 3 h)*

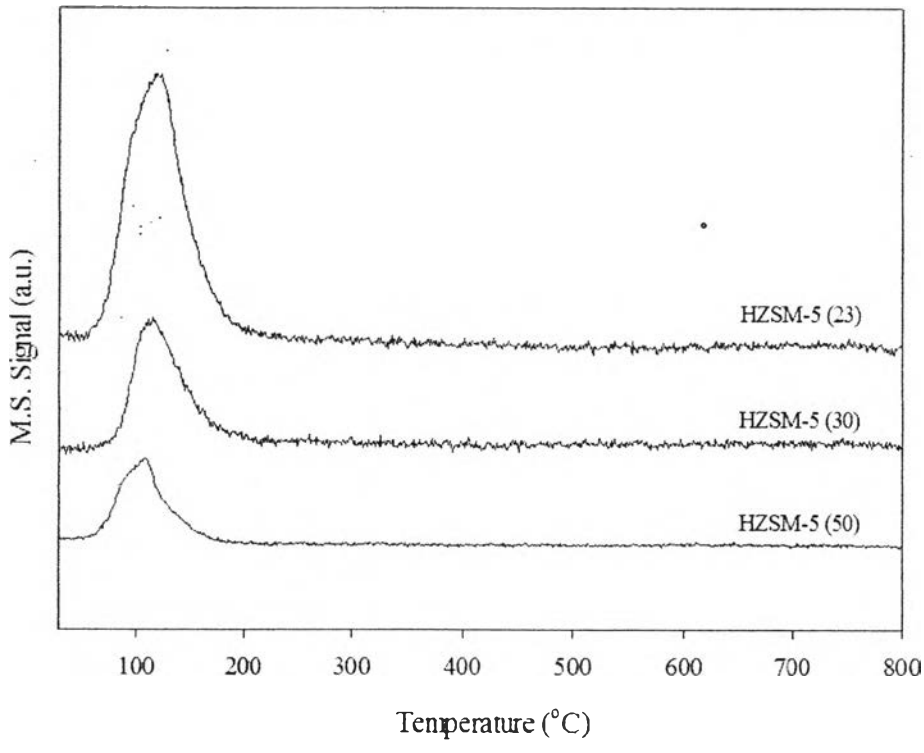

Figure 4.12 H_2O-TPD profiles of the HZSM-5 with SiO_2/Al_2O_3 ratios of 23, 30, and 50. The mass monitored was *m/e* equal 18.

4.2.3 Effect of Metal Loading

To enhance the BTEX yield, the HZSM-5 (30) was selected to further modification by incorporated Zn and Ga species.

4.2.3.1 Effect of Zn Loading

In order to improve the BTEX yield, Zn was loaded on the HZSM-5 (30) zeolite by incipient wetness impregnation (IWI) method. The Zn/HZSM-5 catalysts were studied in the aromatization of PFAD at 500 °C and 1 atm. The conversion was almost 100% for all modified catalysts. The enhancement in BTEX yield and suppression in light paraffins was observed over Zn/HZSM-5 catalysts as shown in Figure 4.13. As Zn loading increased, the formation of paraffins tended to decrease while the formation of aromatics increased (Fanchiang, W.L., 2012). It could be concluded that the introducing of Zn species exchanged with strong Brønsted acid site remarkably enhanced the aromatics formation by following

two reasons. First, the presence of Zn replacing the strong Brønsted acid which suppressed the hydrogen transfer reaction thus enhanced the reactions towards aromatics (Fanchiang, W.L., 2012). Second, the bivalent Zn cations at the exchanged site had a high capacity in dehydrogenation reaction, enhancing the aromatics formation (Tamiyakul, S., 2015). Compared with the parent HZSM-5 (30), Zn/HZSM-5 catalyst greatly improved the hydrogen yield as shown in Figure 4.14. It was also noticed that HZSM-5 (30) exhibited large amount of CO production. The result can be concluded that HZSM-5 (30) catalyzed the decarbonylation reaction. It is accepted that the decarbonylation reaction was performed by the strong acid sites of HZSM-5 catalyst (Ausavasukhi, A., 2009). Otherwise, Zn/HZSM-5 catalysts promoted the formation CO_2 (Sugiyama, S., 1992) with the decrease of CO production. We believed that the decrease in the Brønsted acid site (Table 4.3) and the presence of ZnO species (Table 4.4) shifted the deoxygenation pathway from decarbonylation to decarboxylation (Fanchiang, W., 2011). The 5/Zn/HZSM-5 exhibited the highest BTEX yield (65.8 wt%) (Figure B1). The incorporation between the exchangeable Zn^{2+} and ZnO species enhanced the BTEX yield by the following manners. First, the exchangeable Zn^{2+} species enhanced the dehydrogenation reaction thus suppress the hydrogen transfer. Second, the ZnO species promoted the decarboxylation reaction. Consequently, the strong Brønsted acid site was preserved to aromatization reaction. On the other hand, the further increase in Zn loading from 5 to 7 wt% did not improve the BTEX yield. The reason for that might be due to the partially blocked pore of HZSM-5 zeolite by ZnO species (Table 4.2).

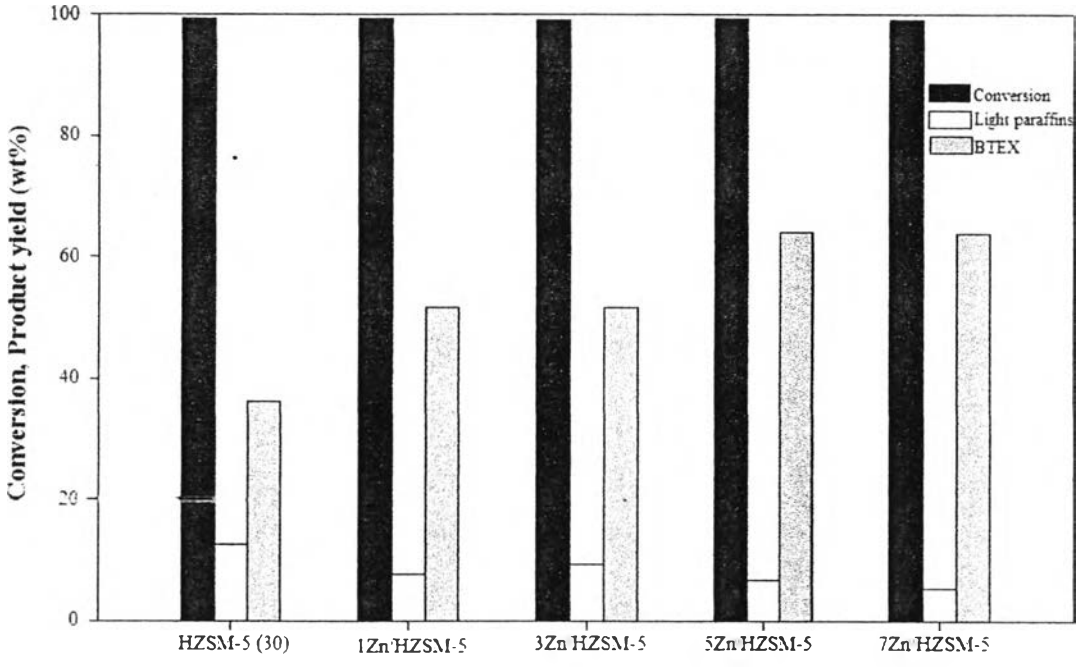

Figure 4.13 Effect of Zn loading on HZSM-5 zeolite on the PFAD conversion, and product yield. *(Reaction conditions: 500 °C under atmospheric pressure, WHSV= 5 h^{-1}, and TOS = 3 h)*

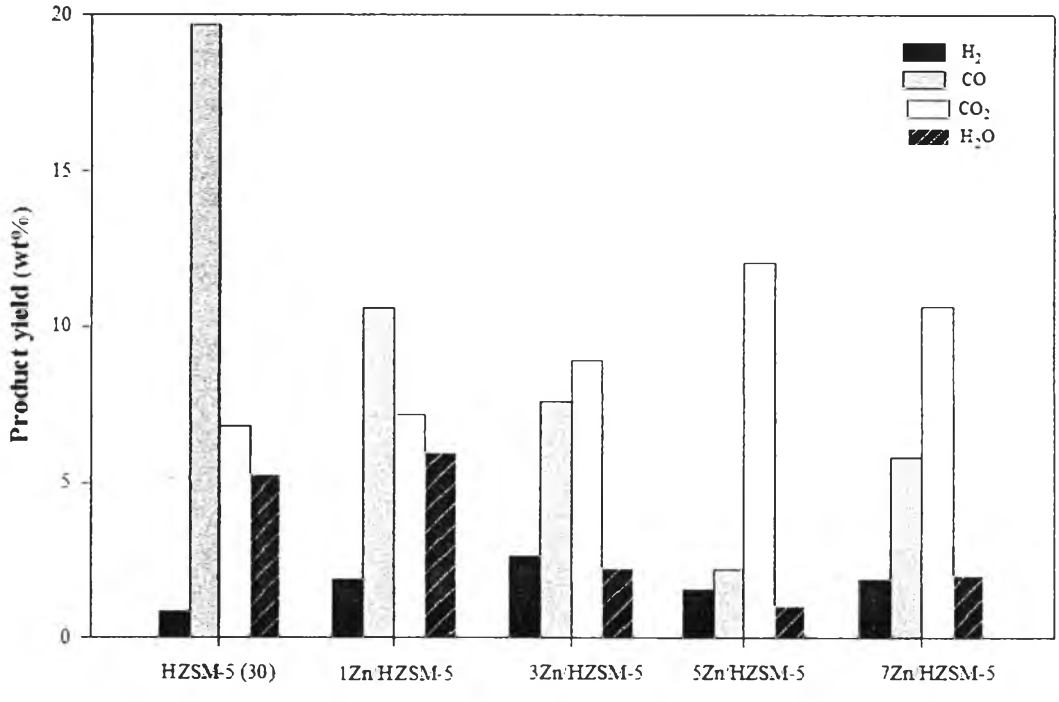

Figure 4.14 Product yield of CO, CO_2, H_2 and H_2O over Zn/HZSM-5 catalysts. *(Reaction conditions: 500 °C under atmospheric pressure, WHSV= 5 h^{-1}, and TOS = 3 h)*

4.2.3.2 Effect of Ga Loading

The enhanced BTEX yield was observed after loading 1 wt% Ga on HZSM-5 catalyst as showed in Figure 4.15. However, it was found that the further increase in Ga loading not improving in the BTEX selectivity. The reason for that might relate to the active species of Ga, improving dehydrogenation activity is the Ga at exchange site (Choudhary, V.R. *et al*, 2000). The products from the deoxygenation reaction of PFAD over Ga/HZπSM-5 catalysts were illustrated in Figure 4.16, the results were apparently same as HZSM-5 (30) catalyst. HZSM-5 (30) and Ga/HZSM-5 catalyzed the decarbonylation reaction, the active site for this reaction was the strong Brønsted acid site, resulting in high amount of CO production (Ausavasukhi, A., 2009., Dao *et al*, 1987., and Haniff, M.I., 1988). As the Ga loading increase, the strong Brønsted acidity trend to decrease (Table 4.3) resulted in lower decarbonylation activity and lower CO production.

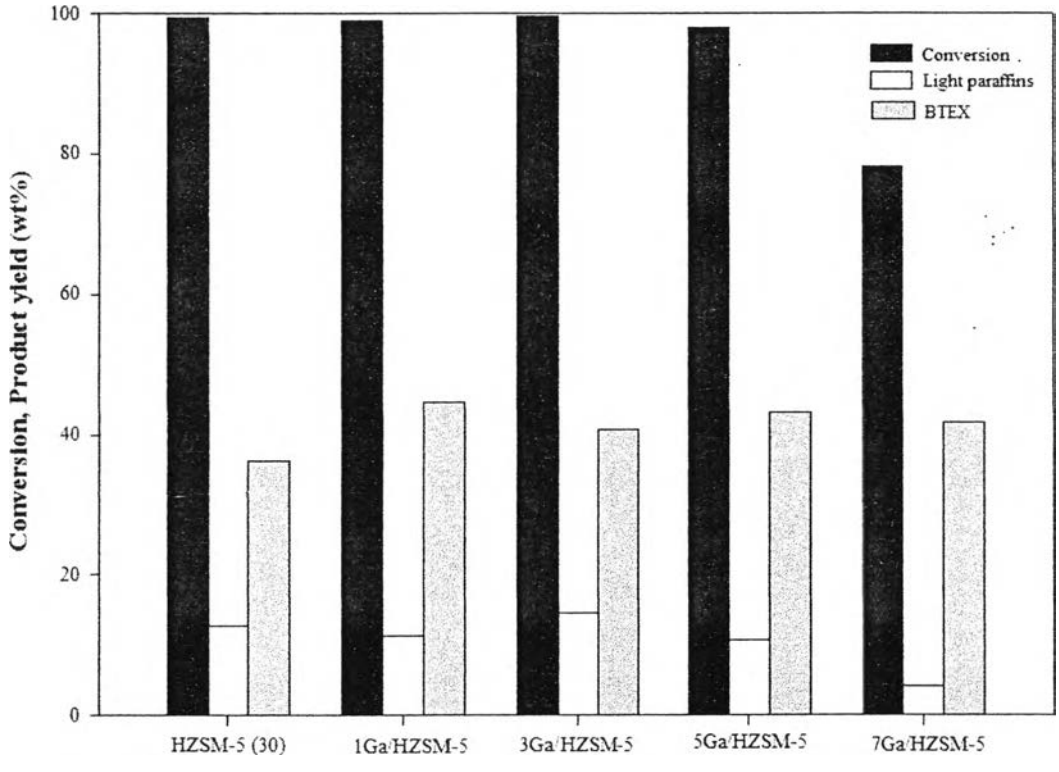

Figure 4.15 Effect of Ga loading on HZSM-5 zeolite on the PFAD conversion, and product yield. *(Reaction conditions: 500 °C under atmospheric pressure, WHSV= 5 h^{-1}, and TOS = 3 h)*

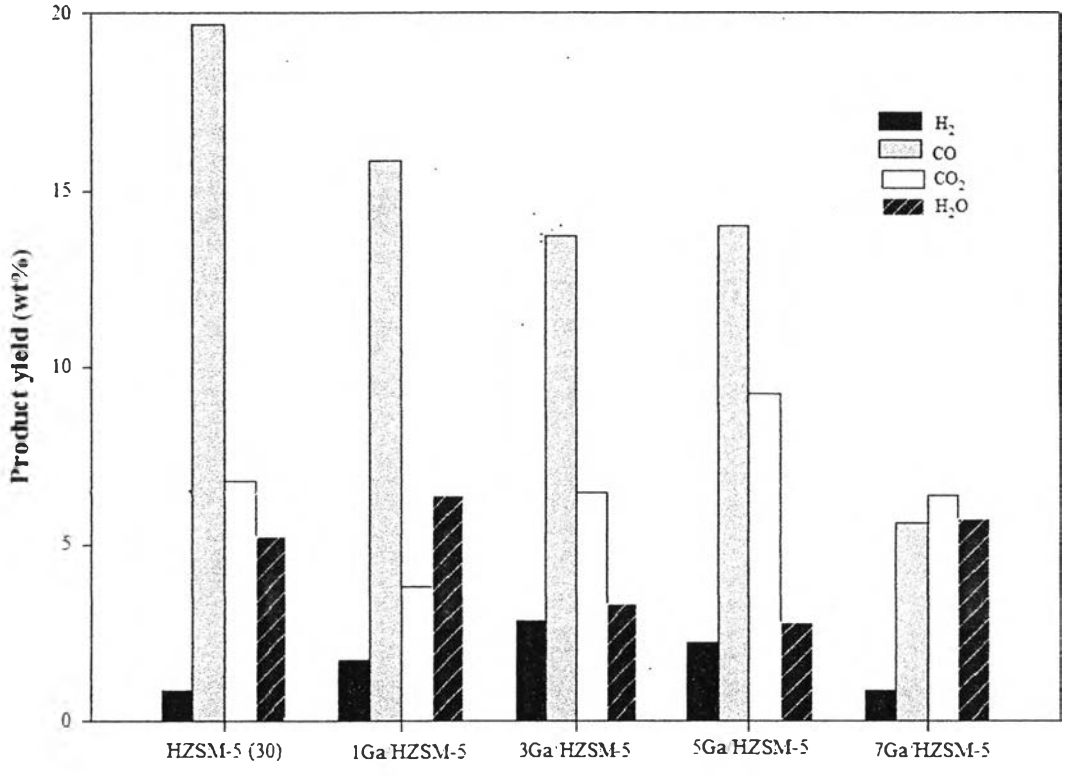

Figure 4.16 Product yield of CO, CO_2, H_2 and H_2O over Ga/HZSM-5 catalysts. *(Reaction conditions: 500 °C under atmospheric pressure, WHSV= 5 h^{-1}, and TOS = 3 h)*

The presence of Zn and Ga species on parent HZSM-5 (30) could enhance the BTEX yield. For Zn/HZSM-5 catalysts enhanced the BTEX yield by following manners. First, the bivalent Zn cations at exchange site decreased the strong Brønsted acidity (Table 4.3) thus suppressed the multiple oligomerization cracking steps and enhanced the dehydrogenation reaction by recombinative desorption of H atoms to H_2 molecule (Lili Yu *et al.*, 2012). Second ZnO species promoted decarboxylation (Haniff, M.I., 1988., and Dmitri, A., 2010), shift the deoxygenation reaction from decarbonylation to decarboxylation thus the strong Brønsted acid site was preserved to aromatization activity. For Ga/HZSM-5 catalysts, the increase of Ga loading did not improve BTEX yield. Because Ga_2O_3 species was found to be ineffective as catalysts for aromatization of PFAD.